CMI

www.nature.com/cmi

ARTICLE

Inhibition of CD82 improves colitis by increasing NLRP3 deubiquitination by BRCC3

Jae-Sung Kim[1,2], Hyo Keun Kim[3,4], Joongho Lee[5], Sein Jang[3,4], Euni Cho[1,4], Seok-Jun Mun[1,4], Seokhyun Yoon[6] and Chul-Su Yang[3,4]✉

CD82 is a transmembrane protein that is involved in cancer suppression and activates immune cells; however, information on the NLRP3 inflammasome is limited. Herein, we show that although CD82 suppressed the activation of the NLRP3 inflammasome in vivo and in vitro, CD82 deficiency decreased the severity of colitis in mice. Furthermore, two binding partners of CD82, NLRP3 and BRCC3, were identified. CD82 binding to these partners increased the degradation of NLRP3 by blocking BRCC3-dependent K63-specific deubiquitination. Previous studies have shown that CD82-specific bacteria in the colon microbiota called *Bacteroides vulgatus* (*B. vulgatus*) regulated the expression of CD82 and promoted the activation of the NLRP3 inflammasome. Accordingly, we observed that *B. vulgatus* administration increased mouse survival by mediating CD82 expression and activating NLRP3 in mice with colitis. Overall, this study showed that CD82 suppression reduced the pathogenesis of colitis by elevating the activation of the NLRP3 inflammasome through BRCC3-dependent K63 deubiquitination. Based on our findings, we propose that *B. vulgatus* is a novel therapeutic candidate for colitis.

Keywords: CD82; NLRP3; BRCC3; Colitis; Inflammation

Cellular & Molecular Immunology (2023) 20:189–200; https://doi.org/10.1038/s41423-022-00971-1

INTRODUCTION

CD82, also known as KAI1, is a member of the tetraspanin superfamily. It comprises four transmembrane domains and suppresses cancer metastasis. Studies have suggested that differentially expressed KAI1/CD82 is closely related to malignant tumors and can be measured as a tumor biomarker [1, 2]. Notably, KAI1/CD82 expression is downregulated in malignant tumors and closely associated with malignant progression, metastasis, and prognosis particularly in breast, colon, lung, ovarian, nasopharyngeal, liver, and pancreatic cancers [3–5]. Additionally, KAI1/CD82 has been found to be related to diverse biological functions, such as cell signal transduction, adhesion, migration, and motility and protein trafficking, and aggregation [6]. Moreover, studies have indicated that although immuno-crosslinking of KAI1/CD82 induces intracellular calcium mobilization in lymphocytes, T-cell adhesion and the level of KAI1/CD82 on the cell surface are upregulated during cell activation and cytokine stimulation, with KAI1/CD82 playing an accessory role in T-cell activation [7–9]. Alternately, although CD82 has been associated with components of the major histocompatibility complex (MHC) class II antigen presentation pathway, such as class II MHC molecules and peptide-loading machinery, it is also specifically recruited to pathogen-containing phagosomes before fusion with lysosomes in macrophages, indicating roles for CD82 in antigen presentation and intracellular trafficking in macrophages [10, 11]. However, neither the involvement of CD82 expression in colitis pathogenesis nor the mechanisms by which CD82 is associated with inflammation-related protein regulation in macrophages are well understood.

The nucleotide-binding oligomerization domain-like receptor pyrin-domain containing protein 3 (NLRP3) inflammasome is the most extensively characterized crucial signaling factor that influences the maturation of two proinflammatory interleukin (IL)-1 family cytokines, namely, IL-1β and IL-18 [12, 13]. Activating pattern recognition receptors, NLRP3 forms a homogenous complex called the adapter apoptosis-associated speck-like protein containing a caspase recruitment domain (ASC). This complex, in turn, activates pro-caspase-1 via its cleavage. Caspase-1 is a well-characterized inflammatory caspase that facilitates the maturation of IL-1β and IL-18 into active cytokines and the initiation of pyroptosis by autocatalysis and activation [14–16]. Furthermore, it initiates gene transcription, particularly the priming step, triggering the expression of NLRP3, pro-IL-1β, and pro-IL-18 in preparation for inflammasome activation [17, 18]. Then, various stimuli, such as uric acid crystals, cholesterol, silica, alum, ATP, and calcium pyrophosphate dehydrate [18–20], induces NLRP3 inflammasome activation. Hence, the activation of the NLRP3 inflammasome has been proposed to be regulated at both the transcriptional and posttranslational levels.

[1]Department of Bionano Technology, Hanyang University, Seoul 04673, Korea. [2]Institute of Natural Science & Technology, Hanyang University, Ansan 15588, Korea. [3]Department of Molecular and Life Science, Hanyang University, Ansan 15588, Korea. [4]Center for Bionano Intelligence Education and Research, Ansan 15588, Korea. [5]Department of Computer Science, College of SW Convergence, Dankook University, Yongin 16890, Korea. [6]Department of Electronics & Electrical Engineering, College of Engineering, Dankook University, Yongin 16890, Korea. ✉email: chulsuyang@hanyang.ac.kr

Received: 15 June 2022 Accepted: 21 December 2022
Published online: 5 January 2023

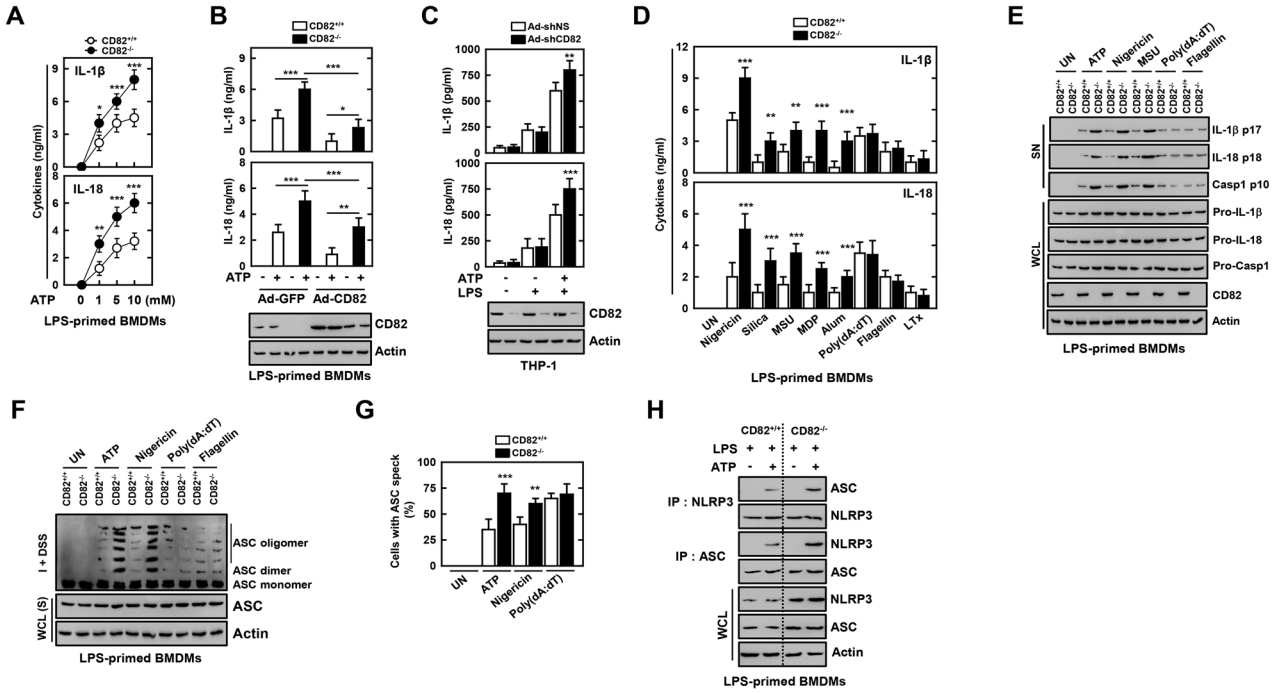

Fig. 1 Inflammasome in macrophages A BMDMs from CD82$^{+/+}$ and CD82$^{-/-}$ mice were primed with LPS (100 ng/mL) for 4 h and stimulated with ATP at various concentrations for 1 h. The levels of cytokines were analyzed by ELISAs for IL-1β and IL-18. **B**, **C** BMDMs were transduced with Ad-GFP or Ad-CD82 at 200 PFU/cell for 48 h (**B**, upper). THP-1 cells were transduced with Ad-shNS or Ad-shCD82 at 200 PFU/cell for 48 h (**C**, upper). The experimental conditions were based on the protocol outlined in (**A**). Whole cell lysates (WCLs) were used for IB with αCD82, and αActin was used as the loading control (lower). **D**, **E** BMDMs from CD82$^{+/+}$ and CD82$^{-/-}$ mice were primed with LPS and stimulated with nigericin, silica, MSU, MDP, alum, poly(dA:dT), flagellin or LTX for 1 h. **D** ELISAs for IL-1β and IL-18. **E** IB in supernatant (SN) with αIL-1β p17, αIL-18 p18 or αCasp1 p10 and WCL with αPro-IL-1β, αPro-IL-18, αPro-Casp1, or αActin. **F** IB of lysates of BMDMs was performed as shown in **E** and solubilized with Triton X-100-containing buffer, followed by cross-linking insoluble fractions with disuccinimidyl suberate to capture ASC oligomers for analysis of these fractions (I + DSS) and the soluble fractions (S) with αASC. αActin was used as the loading control. **G** Fluorescence confocal images showing the formation of speck-like ASC pyroptosomes in BMDMs after fixation and immunostaining with antibodies for ASC (Alexa 488). The data are representative of five independent experiments with similar results. **H** BMDMs were subjected to IP with αNLRP3 or αASC, followed by IB with αASC or αNLRP3. WCLs were used for IB with αNLRP3, αASC or αActin. Data shown are the means ± SDs of three experiments (**A**–**D**, **G**). The data are representative of four independent experiments with similar results (**B**, **C**, **E**, **F**, and **H**). Statistical significance was determined by Student's *t*-test with Bonferroni adjustment (*$p < 0.05$, **$p < 0.01$, ***$p < 0.001$) compared with CD82$^{+/+}$ (**A**–**D**, **G**)

The NF-kB pathway induces NLRP3, pro-IL-1β, and pro-IL-18 expression at the transcriptional level. Before stimulation, the inactive conformation of NLRP3 is partially formed by several posttranslational modifications, such as phosphorylation and ubiquitylation [14, 21–23]. Ubiquitylation modulates NLRP3 activation by controlling both the degradation rate of NLRP3 and its ability to self-assemble. Notably, BRCA1/BRCA2-containing complex subunit 3 (BRCC3) is a deubiquitinase activated by priming signals, and it deubiquitylates NLRP3 to enable its homo-oligomerization [24, 25]. However, the role played by CD82, which has been associated with BRCC3 and NLRP3 in macrophages, remains unclear.

Aberrant activation of the NLRP3 inflammasome is evident in various autoinflammatory and chronic inflammatory and metabolic diseases, including gout, atherosclerosis, and type 2 diabetes [14, 16]. Early studies reported that the NLRP3 inflammasome produces IL-1β and IL-18, contributing to intestinal inflammation [26, 27]. However, aberrant inflammasome signaling in inflammatory bowel disease (IBD) is being re-evaluated due to recent reports indicating that IL-1β and IL-18 production can confer protection against colitis [28–30].

Based on the background described above, the aim of this study was to investigate the role played by CD82 in DSS-induced colitis in mice. To this end, this study proved that the regulation of CD82 may be a potential target for colitis therapeutics. The results showed that CD82 interacted with NLRP3 and BRCC3. Furthermore, with the binding of BRCC3-CD82, a decrease in the K63-specific deubiquitination of NLRP3 led to increased NLRP3 degradation and thus attenuated NLRP3 inflammasome activation. Subsequently, we studied the role played by *Bacteroides vulgatus* (*B. vulgatus*), which has been associated with probiotics in the colon, in decreasing the susceptibility to colitis. The oral administration of *B. vulgatus* to mice with DSS-induced colitis attenuated the expression and binding of CD82 following enhanced activation of the NLRP3 inflammasome.

RESULTS

CD82 inhibits the activation of the NLRP3 inflammasome

We treated LPS-primed wild-type (WT) or CD82-knockout (KO) BMDMs with various concentrations of ATP to examine the role of CD82 in activating the NLRP3 inflammasome. Then, we measured the levels of secreted IL-1β and IL-18. These investigations revealed that the levels of the aforementioned cytokines were increased in CD82-deficient BMDMs compared to WT BMDMs (Fig. 1A).

However, in a complementary experiment, CD82 decreased the levels of cytokines in both mutant and WT BMDMs infected with adenovirus (Fig. 1B). Knocking down CD82 favored the expression of IL-1β and IL-18 in THP-1 cells (Fig. 1C). Subsequently, we analyzed the effects various inflammasome activators in LPS-primed WT and CD82$^{-/-}$ BMDMs to determine whether CD82 specifically mediates NLRP3 inflammasome activity. Although treatment with NLRP3 activators (nigericin, silica, MSU, MDP, or alum) significantly elevated

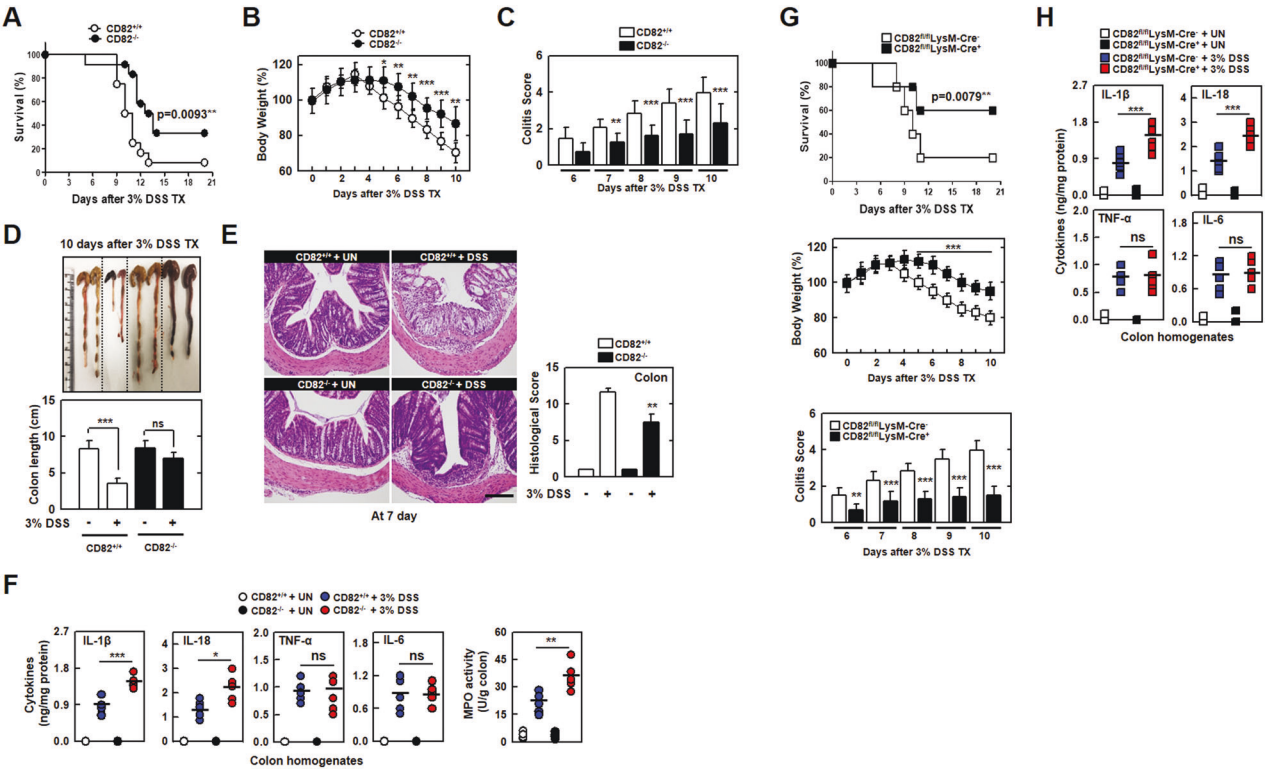

Fig. 2 CD82 deficiency led to activated NLRP3-dependent responses in vivo A The acute colitis model mice treated with 3% DSS for 5 days. The survival of the mice was monitored for 21 days; mortality was measured for $n = 12$ mice per group. Statistical differences compared with the $CD82^{+/+}$ mice are indicated (log-rank test). The data are representative of three independent experiments with similar results. **B** Weight loss ($n = 10$). **C** Colitis scores were obtained on the basis of the clinical parameters (weight loss, stool consistency, and bleeding) ($n = 10$). **D** Image (upper) and length (lower) of the colon in 3% DSS-treated mice ($n = 8$). **E** Representative image showing hematoxylin and eosin (H&E) staining of the colon (left) ($n = 10$). Histopathology scores for 3% DSS-treated mice (right) were obtained on the basis of H&E staining as described in the Methods (Materials and Methods). Scale bar, 200 μm. **F** The levels of cytokines and the MPO activity in colon homogenates ($n = 10$). **G**, **H** $CD82^{fl/fl}$ LysM-Cre+ and $CD82^{fl/fl}$ LysM-Cre- mice were treated with 3% DSS for 5 days. **G** The survival of the mice was monitored for 21 days on the basis of weight loss and colitis scores ($n = 15$). **H** The levels of cytokines in colon homogenates ($n = 10$). Statistical significance was determined by Student's *t*-test with Bonferroni adjustment (*$p < 0.05$; **$p < 0.01$, ***$p < 0.001$) compared with $CD82^{+/+}$ or $CD82^{fl/fl}$ LysM-Cre- mice

the levels and secretion rates of IL-1β and IL-18, they did not affect the levels of AIM2 (poly(dA:dT)), NLRC4 (flagellin), or NLRP1 (LTx) activators in the BMDMs (Fig. 1D, E). Furthermore, although the oligomerization of ASC was significantly increased after treatment of $CD82^{-/-}$ BMDMs with an NLRP3 activator compared to its effect on WT BMDMs, this increase was not observed with the other inflammasome activators (Fig. 1F, G). Moreover, the binding of NLRP3 and ASC was increased in the LPS-primed CD82-KO BMDMs (Fig. 1H). Interestingly, the function of CD82 in TLR4 signaling was not different between the macrophages of $CD82^{+/+}$ and $CD82^{-/-}$ mice (Fig. S1). Altogether, these results show that CD82 negatively regulates the activation of the NLRP3 inflammasome in macrophages.

CD82 deficiency led to increased survival of mice with DSS-induced colitis

Ulcerative colitis (UC) is a severe inflammatory disease of the colon. Since the pathogenesis of UC has been closely related to NLRP3 inflammasome activation [14, 27], we examined the association of CD82-NLRP3 in mice with DSS-induced colitis. The results showed that the deletion of CD82 protected mice against DSS-induced colitis (Fig. 2A). Weight loss peaked at approximately 20% in $CD82^{-/-}$ mice with DSS-induced colitis (Fig. 2B). Furthermore, the colitis score was significantly reduced in the $CD82^{-/-}$ mice (Fig. 2C), and the length of the mouse colon was largely recovered within 10 days in the CD82-deficient mice after DSS treatment (Fig. 2D). Next, we evaluated the histological scores of mouse colon tissue samples after 7 days. In the DSS-treated mouse colon, the histological score was lower in $CD82^{-/-}$ mice than in the WT mice (Fig. 2E). We also examined cytokine levels and myeloperoxidase (MPO) activity in colon homogenates. The levels of IL-1β and IL-18 expression and MPO activity were increased in the DSS-treated $CD82^{-/-}$ mice (Fig. 2F).

Additionally, disease phenotypes were analyzed in detail (Fig. S2). First, the populations of macrophages and dendritic cells, but not the T-cell population, including Tregs, in the colon, were significantly increased in the mice with DSS-induced colitis $CD82^{-/-}$ compared with the $CD82^{+/+}$ mice (Fig. S2A). Second, anti-inflammatory responses (as indicated by IL-10 and TGF-β levels) were significantly increased in $CD82^{-/-}$ mice with DSS-induced colitis (Fig. S2B). Thus, the inflammation-modulating action of the CD82 protein seemed to act primarily in macrophages. Third, we analyzed the polarization of macrophages and confirmed that M1 macrophage differentiation was decreased and that M2 macrophage differentiation was increased in the $CD82^{-/-}$ mice with DSS-induced colitis (Fig. S2C). However, matrix metalloproteinase-2 and -9 expression was involved in epithelial repair and wound healing in the DSS-induced colitis mice (Fig. S2D), and the gasdermin-mediated pyroptosis rate of macrophages was not different between the $CD82^{+/+}$ and $CD82^{-/-}$ mice in mice with colitis (Fig. S2E). Consistent with the data shown in Fig. 2A–F, macrophage-specific CD82 KO ($CD82^{fl/fl}$LysM-Cre^{+}) increased the survival, body weight, colitis scores, and cytokine expression (IL-1β and IL-18) of mice with DSS-

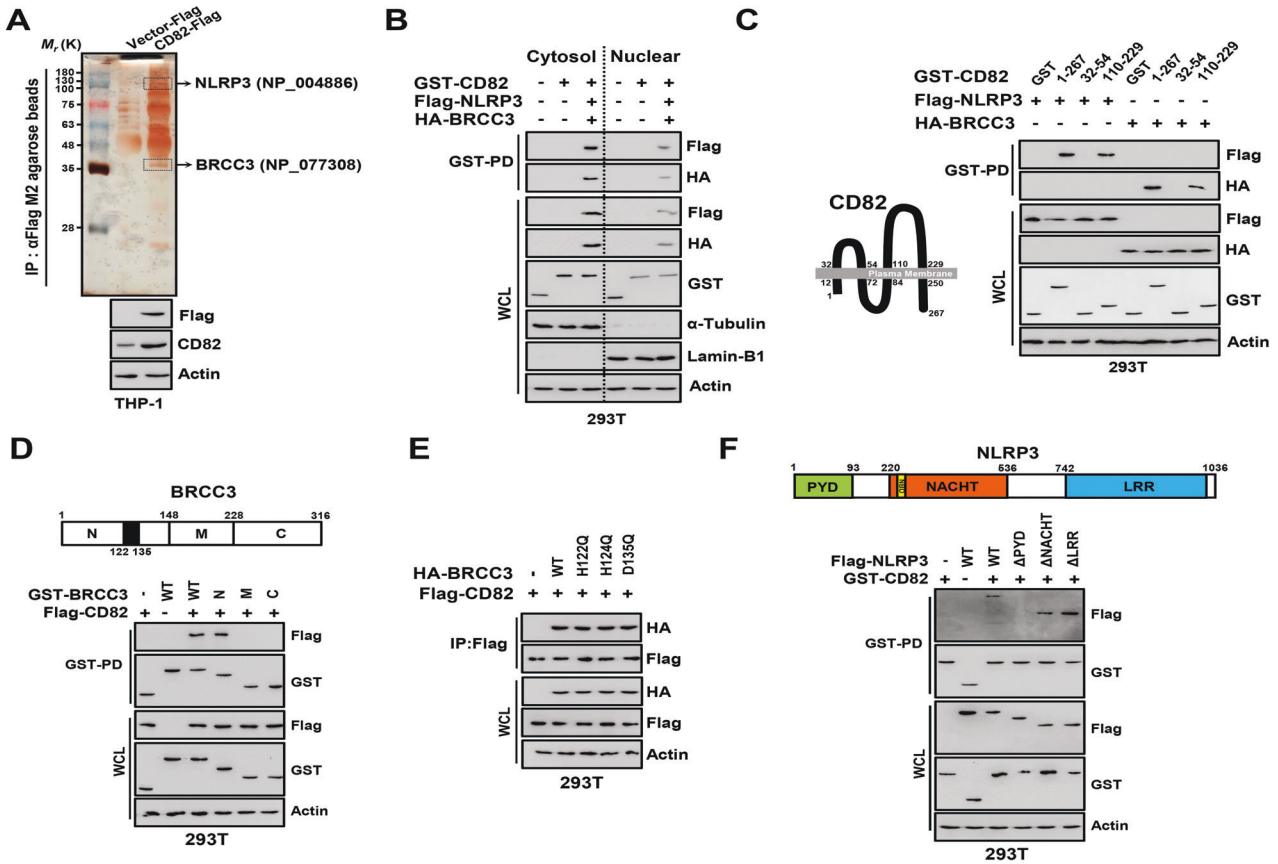

Fig. 3 CD82 directly binds with NLRP3 or BRCC3 A Identification of NLRP3 and BRCC3 as endogenous binding partners of CD82. THP-1 cell lysates were incubated with Flag-tagged CD82 or a vector and then subjected to IP with Flag M2-agarose beads. Binding partners were confirmed by silver staining and mass spectrometric analysis. The peptides identified by mass spectrometry analysis are shown in Fig. S3. **B** 293 T cells were cotransfected with GST-CD82 with Flag-NLRP3 and HA-BRCC3, and then, nuclear and cytoplasmic fractions were separated and subjected to GST pulldown assay, followed by IB with αFlag and αHA antibodies. WCLs were used for IB with an αFlag, αHA, αGST or αActin antibody. αTubulin was measured as the cytoplasmic protein loading control. αLamin B1 was measured as the nuclear loading control. **C** Schematic diagram of the structures of CD82 (left). 293 T cells were cotransfected with Flag-NLRP3 and HA-BRCC3 together with a GST-vector or GST-CD82 and its mutant constructs (right). The experimental conditions were based on the protocol outlined in (**B**). **D** Schematic diagram of the structures of BRCC3 (upper). 293 T cells were cotransfected with Flag-CD82 together with a GST-vector or GST-BRCC3 and its mutant constructs and subjected to GST pulldown assay, followed by IB with an αFlag antibody. WCLs were used for IB with an αGST, αFlag or αActin antibody (lower). **E** 293 T cells were cotransfected with Flag-CD82 together with a HA-vector or HA-BRCC3 and its mutant constructs and subjected to IP with an αFlag antibody, followed by IB with an αHA antibody. WCLs were used for IB with an αHA αFlag or αActin antibody. **F** Schematic diagram of the structures of NLRP3 (upper). 293 T cells were cotransfected with GST-CD82 together with a Flag-vector or Flag-NLRP3 and its mutant constructs and subjected to GST pulldown assay, followed by IB with an αFlag antibody. WCLs were used for IB with an αGST, αFlag or αActin antibody (lower). The data are representative of four independent experiments with similar results

induced colitis (Fig. 2G, H). Therefore, our findings show that enhancing the NLRP3 inflammasome by reducing macrophage-specific CD82 levels decreased the pathogenesis rate of colitis in mice.

CD82 interacts with NLRP3 and BRCC3

Subsequently, we examined the interplay of CD82 with other molecules involved in NLRP3 inflammasome activation to establish a role for CD82 in activating the NLRP3 inflammasome in macrophages. First, we overexpressed Flag-tagged CD82 in THP-1 macrophages and performed coimmunoprecipitation (co-IP) with a Flag antibody. These results led to the identification of CD82 binding, which included NLRP3 (118 K) and BRCC3 (36 K), via mass spectrometry (Fig. 3A and S3). Then, to investigate the subcellular localization of the NLRP3-CD82-BRCC3 complex, we examined its subcellular localization in 293 T cells by overexpressing CD82, NLRP3, and BRCC3, and then performed a GST pulldown (GST-PD) assay with cytosolic and nuclear fractions. In both fractions, CD82 interacted with NLRP3 and BRCC3. In particular, the interaction of CD82 with NLRP3 or BRCC3 was strongest in the cytosolic fraction (Fig. 3B). Therefore, we further investigated the domains in NLRP3 and BRCC3 that interact with CD82 by overexpressing full-length GST-tagged WT CD82, a small extracellular loop (SEL, 32–54), and a long extracellular loop (LEL, 110–229) region of CD82 with Flag-tagged NLRP3 or HA-tagged BRCC3 in 293 T cells. In the GST-PD assay, both NLRP3 and BRCC3 were associated with the CD82 LEL region, which suggested that the LEL was essential for the NLRP3 and BRCC3 interaction (Fig. 3C). Additionally, we examined the ability of a fundamental domain in BRCC3 to interact with CD82 by analyzing BRCC3 truncation mutants. We thus identified that the N-terminus of BRCC3 was an indispensable domain that favored binding to CD82 (Fig. 3D).

Alternatively, studies have reported that BRCC3 carries three metal-binding sites, namely, histidine (H) 122, 124, and aspartic acid (D) 135, which are related to metalloprotease activity and DNA repair function [31–33]. Therefore, we investigated whether these amino acids were needed to interact with BRCC3 and CD82 by generating point mutations of the H122, 124, and D135 amino acids, which were replaced with glutamine (Q), to abolish their role in BRCC3 binding. In 293 T cells, the mutations to H122, 124,

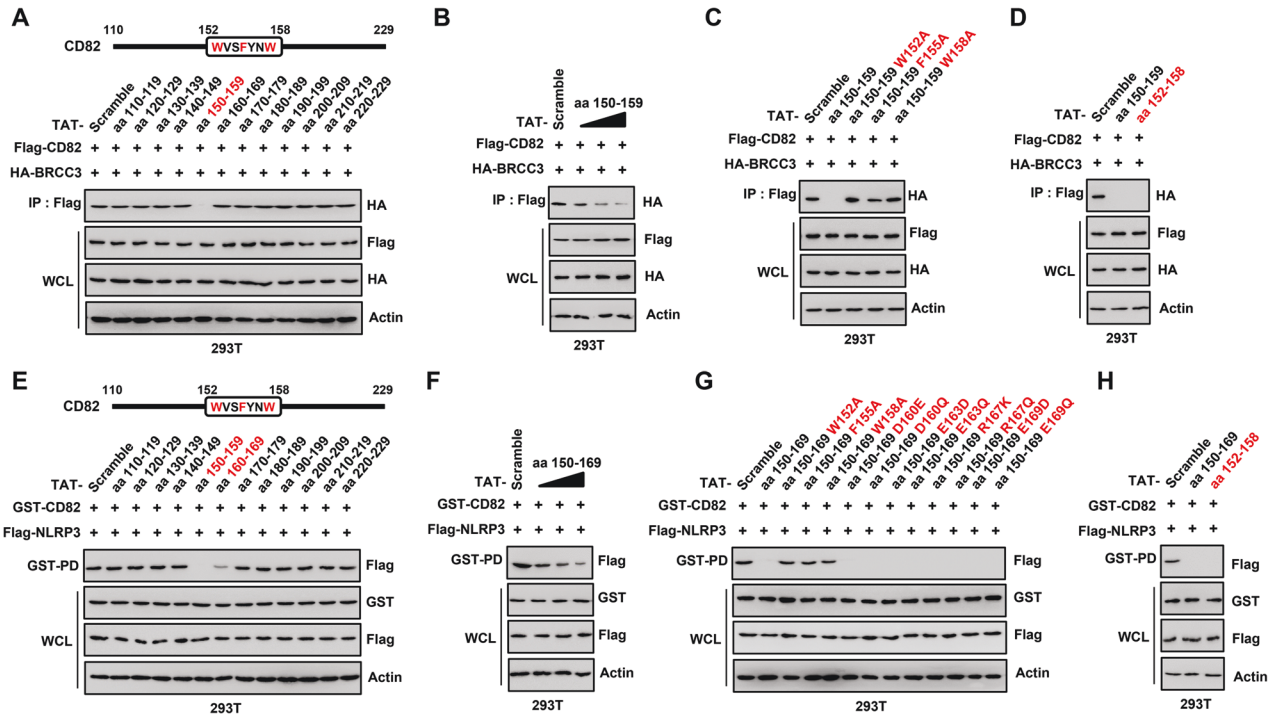

Fig. 4 TAT-CD82 (aa 152-158) is an essential region for binding to NLRP3 and BRCC3 A–D Schematic design of the CD82 peptide and its mutants (**A**, upper). 293 T cells were transfected with Flag-CD82 and HA-BRCC3 and treated with CD82 peptide or its mutants for 6 h (**A**, **C**, and **D** for 5 μM; **B** for 1, 5, 10 μM). 293 T cells were used for IP with an αFlag antibody, followed by IB with an αHA antibody. WCLs were used for IB with an αFlag, αHA and αActin antibody. **E–H** 293 T cells were transfected with GST-CD82 and Flag-NLRP3 and treated with CD82 peptide or its mutants for 6 h (**E**, **G,** and **H** at 5 μM; **F** at 1, 5, 10 μM). 293 T cells were subjected to GST pulldown assay, followed by IB with an αFlag antibody. WCLs were used for IB with an αGST, αFlag or αActin antibody. The data are representative of seven independent experiments with similar results

or D135 in BRCC3 did not affect BRCC3-CD82 binding (Fig. 3E). In addition, to identify the essential domain for CD82 binding in NLRP3, we performed GSTPD assays with Flag-NLRP3 WT or truncation mutants and GST-CD82 in 293 T cells. Pyrin domain (PYD)-deficient NLRP3 failed to bind CD82, demonstrating that the PYD domain in NLRP3 was important for the NLRP3 interaction with CD82 (Fig. 3F). Overall, direct binding of NLRP3 to BRCC3, and LEL CD82, including the N-terminal domains in BRCC3 and PYD of NLRP3, was found to be crucial for the direct association of NLRP3 and BRCC3 to CD82.

Amino acids 152–158 in CD82 are essential for binding to NLRP3 and BRCC3

To further study the amino acid (aa) residues in CD82 that interact with NLRP3 and BRCC3, we constructed TAT-GRA8 peptides (separated by ten aas) in the 110-229 region of CD82, after which we subjected the TAT-CD82 peptides in Flag-CD82 and HA-BRCC-expressing 293 T cells to immunoprecipitation with Flag antibodies. Treatment with TAT-CD82 (aa 150–159) disrupted the binding between CD82 and BRCC3, showing that aa 150–159 in CD82 constituted the region for CD82 binding to BRCC3 (Fig. 4A). Subsequently, we added increasing concentrations of TAT-CD82 (aa 150–159) to 293 T cells. CD82-BRCC3 binding in 293 T cells was decreased in a TAT-CD82 (aa 150–159) dose-dependent manner (Fig. 4B). Furthermore, the WXXFXXW motif has been found to be essential for posttranslational modification in several studies [34, 35]. Therefore, to investigate the specific amino acid regions in aa 150–159 of CD82 involved in binding, we introduced point mutations in TAT-CD82 (aa 150–159) at tryptophan (W) 152 and 158 and then replaced phenylalanine (F) 155 with alanine (A). Intriguingly, each point mutation, that is, W152, F155, and W158, in CD82 could not block the interaction between CD82 and BRCC3 (Fig. 4C). This result showed that W152, F155, and W158 in CD82 were essential amino acids for interplay with BRCC3. Subsequently, we produced TAT-GRA8 (aa 152–158), carrying W152, F155, and W158, in 293 T cells to establish minimal amino acids in GRA8 that were related to BRCC3 binding. Consistent with the blockade of CD82-BRCC3 by TAT-CD82 (aa 150–159), TAT- CD82 (aa 152–158) inhibited CD82-BRCC3 binding (Fig. 4D and S4A). Next, we examined the binding region of CD82 with NLRP3 in 293 T cells. Treatment with TAT-GRA8 (aa 150–159) and TAT-GRA8 (aa 160–169) inhibited the GRA8-NLRP3 interaction, and TAT-GRA8 (aa 150–169) decreasedNLRP3 binding to TAT-GRA8 (aa 150–169) in a dose-dependent manner (Fig. 4E, F). In tTAT-GRA8 (aa 150–169), point mutations at W152, F155, and W158 were also determined to be crucial for the CD82-NLRP3 interaction. Point mutations at D160, E163, R167, and E169 exerted no effect on the CD82 binding to NLRP3. Furthermore, the TAT-GRA8 (aa 152–158) peptide blocked the interaction between CD82 and NLRP3, similar to the outcome presented in Fig. 4D (Fig. 4G, H and S4B). These results indicated that aa 152–158 in GRA8 was the region fundamental for CD83 interactions with BRCC3 and NLRP3.

BRCC3 regulates the degradation of NLRP3 through its interaction with CD82

BRCC3 is a positive regulator of the K63-specific deubiquitination of NLRP3. Deubiquitination of NLRP3 prevents the degradation of NLRP3 and promotes its oligomerization to form the NLRP3 inflammasome [24, 25]. Interestingly, the same region in CD82 interacts with NLRP3 and BRCC3. Therefore, to further examine the interaction between CD82, NLRP3, and BRCC3 mechanistically, we cotransfected GST-CD82, Flag-NLRP3, and HA-BRCC3 into 293 T cells and performed a GST PD assay to examine the interaction of these proteins. In the presence of CD82, NLRP3, and BRCC3, the interaction between CD82 and NLRP3 was decreased in a BRCC3-dependent manner. Additionally, NLRP3 was degraded

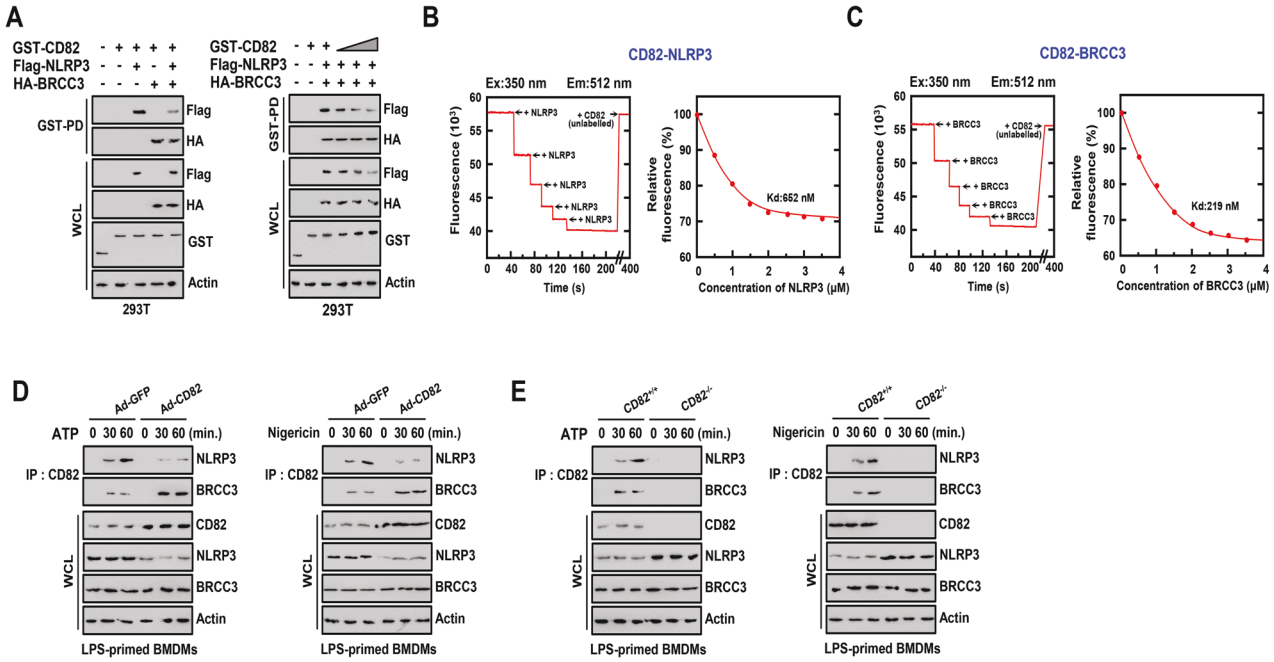

Fig. 5 CD82 regulates the expression of NLRP3 by interacting with BRCC3. A 293 T cells were cotransfected with GST-CD82 together with Flag-NLRP3 or HA-BRCC3 and subjected to GST pulldown assay, followed by IB with αFlag and αHA antibodies. WCLs were used for IB with am αGST, αFlag, αHA or αActin antibody. **B**, **C** Titration of fluorescently labeled NLRP3 with unlabeled CD82 (**B**) with a Kd of 652 nM or fluorescently labeled BRCC3 with unlabeled CD82 (**C**) with a Kd of 219 nM, as determined by curve fit analysis. **D** BMDMs were transduced with Ad-GFP or Ad-CD82 at 200 PFU/cell for 48 h. BMDMs were primed with LPS (100 ng/mL) for 4 h, stimulated with ATP (left, 1 μM) or nigericin (right, 2.5 μM) for 1 h, and subjected to IP with an αCD82 antibody, followed by IB with an αNLRP3 or αBRCC3 antibody. WCLs were used for IB with an αCD82, αNLRP3, αBRCC3 or αActin antibody. **E** BMDMs from $CD82^{+/+}$ and $CD82^{-/-}$ mice were primed with LPS and stimulated with ATP or nigericin. The experimental conditions were based on the protocol outlined in (**D**). The data are representative of five independent experiments with similar results

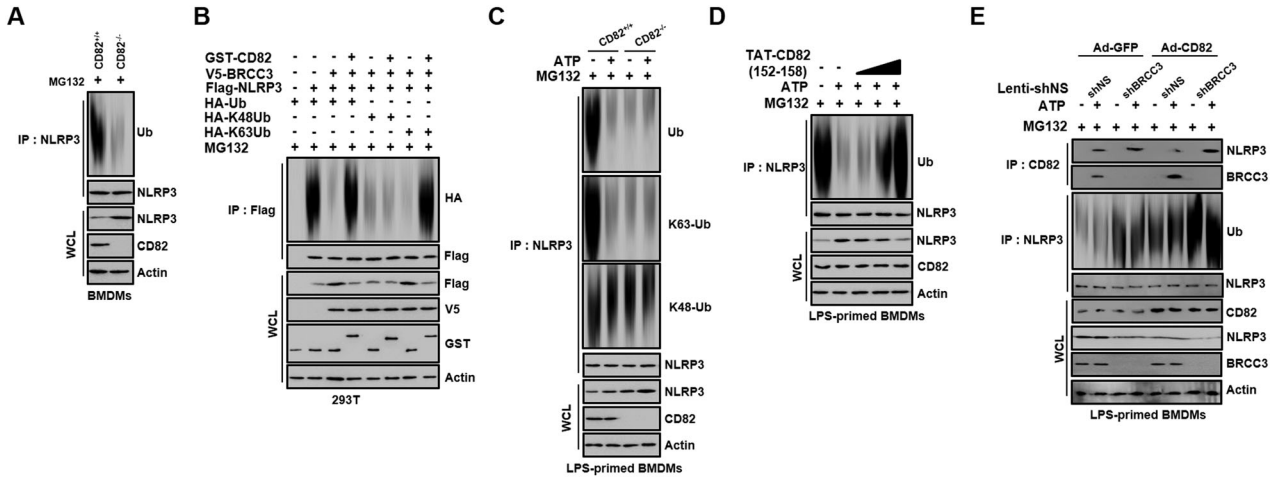

Fig. 6 CD82-BRCC3 binding enhances NLRP3 ubiquitination. A BMDMs were subjected to IP with an αNLRP3 antibody, followed by IB with an αUb or αNLRP3 antibody. WCLs were used for IB with an αCD82, αNLRP3, or αActin antibody. **B** 293 T cells were transfected with GST or GST-CD82, HA-Ub or HA-K48 Ub or HA-K63 Ub, V5-BRCC3 or Flag-NLRP3 in the presence of MG132. After 48 h of transfection, the cells were subjected to IP with an αFlag antibody, followed by IB with an αHA or αFlag antibody. WCLs were used for IB with an αFlag, αV5, αGST or αActin antibody. **C**, **D** The were based on the protocol outlined in (**A**). BMDMs from $CD82^{+/+}$ and $CD82^{-/-}$ mice were primed with LPS and stimulated with ATP in the presence of MG132 (**C**). BMDMs were primed with LPS and stimulated with ATP in the presence of TAT-CD82 (152-158) and MG132 (**D**). **E** BMDMs were transduced with Ad-GFP or Ad-CD82 at 200 PFU/cell for 48 h. BMDMs were transduced with Lenti-NS or Lenti-shBRCC3 at 50 PFU/cell for 48 h. BMDMs were primed with LPS (100 ng/mL) for 4 h and stimulated with ATP, subjected to IP with an αCD82 or αNLRP3 antibody, followed by IB with an αNLRP3, αBRCC3 or αUb antibody. WCLs were used for IB with an αCD82, αNLRP3, αBRCC3 or αActin antibody. The data are representative of five independent experiments with similar results

in BRCC3-co-expressing 293 T cells (Fig. 5A). Subsequently, we performed an in vitro binding assay with fluorescently labeled NLRP3 and BRCC3 and unlabeled CD82 to examine the binding affinity differences between NLRP3 and BRCC3 to CD82. CD82-NLRP3 binding was weaker than that of CD82-BRCC3 (Fig. 5B, C). As a result, we speculated that CD82 might block the deubiquitination of NLRP3 through its interaction with BRCC3. Therefore, we investigated the binding of NLRP3 and BRCC3 with CD82

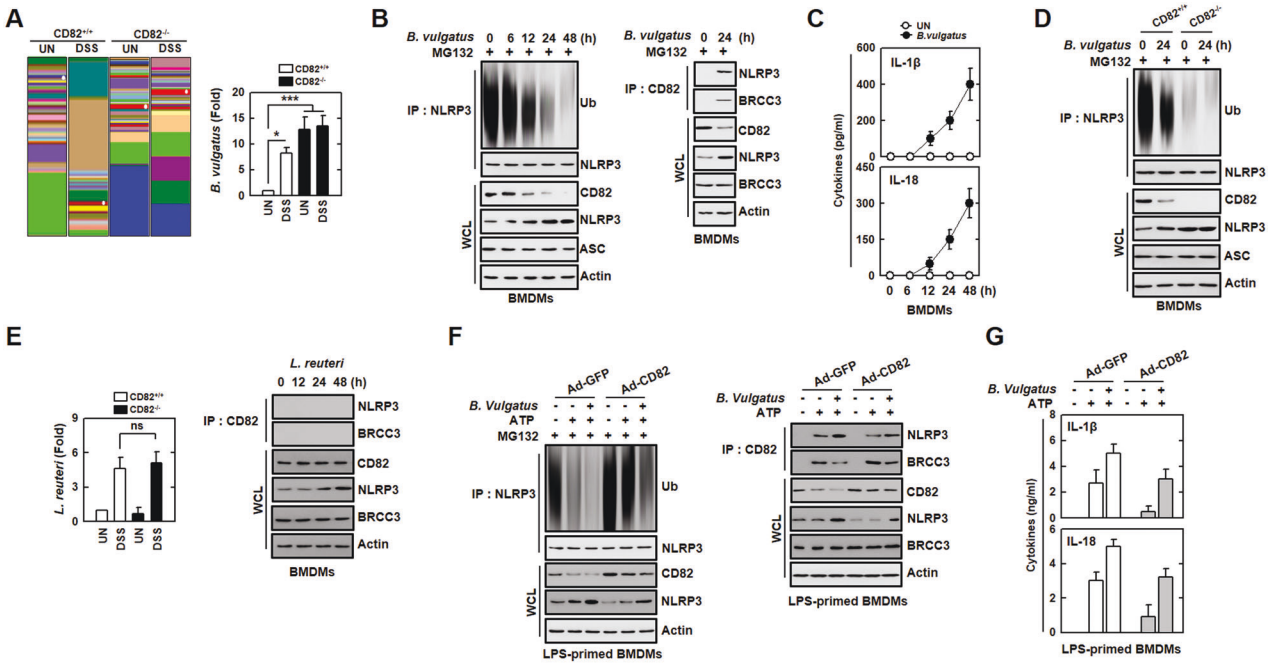

Fig. 7 ***B. vulgatus*** **specifically suppresses the expression and interaction of CD82 with BRCC3 in macrophages A** Gut bacterial composition at the phylum and genus levels by pyrosequencing analysis (left) and the relative abundance of *B. vulgatus* levels (total $n = 4$). **B** BMDMs were infected with *B. vulgatus* (MOI = 20) in the presence of MG132 for the indicated times and subjected to IP with an αNLRP3 (left) or αCD82 antibody (right), followed by IB with an αUb, αNLRP3 or αBRCC3 antibody. WCLs were used for IB with an αCD82, αNLRP3, αASC, αBRCC3 or αActin antibody. **C** The levels of cytokines were analyzed by ELISAs for IL-1β and IL-18. **D** BMDMs from $CD82^{+/+}$ and $CD82^{-/-}$ mice were infected with *B. vulgatus* (MOI = 20) for 24 h in the presence of MG132. The experimental conditions were based on the protocol outlined in (**B**). **E** Relative abundance of *L. reuteri* levels as determined by pyrosequencing analysis (total $n = 4$) (left). BMDMs were infected with *L. reuteri* (MOI = 30) for the indicated times and subjected to IP with an αCD82 antibody, followed by IB with an αNLRP3 or αBRCC3 antibody. WCLs were used for IB with an αCD82, αNLRP3, αASC, αBRCC3 or αActin antibody (right). **F** BMDMs were transduced with Ad-GFP or Ad-CD82. BMDMs were primed with *L. reuteri* for 24 h and stimulated with ATP in the presence of MG132. The experimental conditions were based on the protocol outlined in (**B**). **G** The levels of cytokines were analyzed by ELISAs for IL-1β and IL-18. The data shown are the means ± SDs of three experiments (**C**, **G**). The data are representative of five independent experiments with similar results (**B**, **D**, **E** right, and **F**)

in LPS-primed BMDMs treated with ATP or nigericin. In CD82-overexpressing BMDMs, the binding of NLRP3 with CD82 and the intensity of NLRP3 were decreased compared with those in WT BMDMs (Fig. 5D). Therefore, we further compared the protein level of NLRP3 in LPS-primed WT and $CD82^{-/-}$ BMDMs treated with ATP or nigericin. NLRP3 was increased in $CD82^{-/-}$ BMDMs compared with WT BMDMs (Fig. 5E). Notably, in LPS-coated latex bead-containing endosomal fractions of BMDMs, CD82 interacted with BRCC3 within 30 min and then interacted with NLRP3 within 60 min of challenge with NLRP3-activating stimuli (Fig. S5A). Furthermore, the extracellular loop (aa 110-229) of CD82 interacted with the PYD of NLRP3 or the N-terminus of BRCC3 in the endosome fractions of macrophages (Fig.. S5B–D). Collectively, the CD82 affinity for BRCC3 binding was higher than that for NLRP3 binding, and CD82 increased the degradation of NLRP3 by binding with BRCC3.

CD82 promotes the degradation of NLRP3 by blocking BRCC3-dependent deubiquitination

NLRP3 is regulated by posttranslational modifications such as phosphorylation and ubiquitination. Specifically, it was reported that BRCC3, an NLRP3 regulator, is a deubiquitinase, detaching K63 ubiquitin from a leucine-rich repeat domain in NLRP3 [15]. Therefore, we investigated whether CD82 mediates the BRCC3-dependent deubiquitination of NLRP3 by binding directly to BRCC3. In BMDMs, the ubiquitination rate of NLRP3 was decreased, and NLRP3 levels were increased after CD82 deletion (Fig. 6A). Next, to further examine whether CD82 alleviates the BRCC-dependent K63-specific deubiquitination of NLRP3, we cotransfected plasmids in 293 T cells and immunoprecipitated them with Flag-NLRP3. The results showed that although BRCC3 specifically deubiquitinated K63-ubiquitin on NLRP3, CD82 blocked the deubiquitination of NLRP3 by BRCC3 (Fig. 6B). However, in LPS-primed BMDMs, CD82 deficiency increased the deubiquitination rate of NLRP3. Furthermore, after ATP treatment, NLRP3 was observed to be deubiquitinated in both primed and unprimed BMDMs (Fig. 6C). Specifically, we treated LPS-primed BMDMs with TAT-CD82 (aa 152–158) and ATP, and we found that TAT-CD82 (aa 152–158) increased the ubiquitination and degradation of NLRP3 in a dose-dependent manner (Fig. 6D). Furthermore, BRCC3 played an important role in regulating NLRP3 expression in BRCC3-knockdown macrophages via NLRP3 inflammasome stimuli (Fig. 6E). Considering our results, we established that CD82 negatively controls the BRCC3-dependent K63-specific deubiquitination of NLRP3 by interacting with BRCC3.

B. vulgatus augments the activation of the NLRP3 inflammasome by attenuating CD82 expression in macrophages

We speculated that the composition of microbes in the colon is altered in colitis. Therefore, we analyzed the microbiome in normal and DSS-induced colitis mouse colons using pyrosequencing to verify colon microbiome changes. We observed that the relative abundance of *B. vulgatus* was significantly increased in the colons of the DSS-treated mice. Intriguingly, however, the proportion of *B. vulgatus* was increased in the $CD82^{-/-}$ colon (Fig. 7A). Then, to investigate whether *B. vulgatus* is associated with CD82-NLRP3-BRCC3 binding in macrophages, we infected BMDMs with *B. vulgatus* for the indicated times. Although the ubiquitination of NLRP3 and expression of CD82 were decreased,

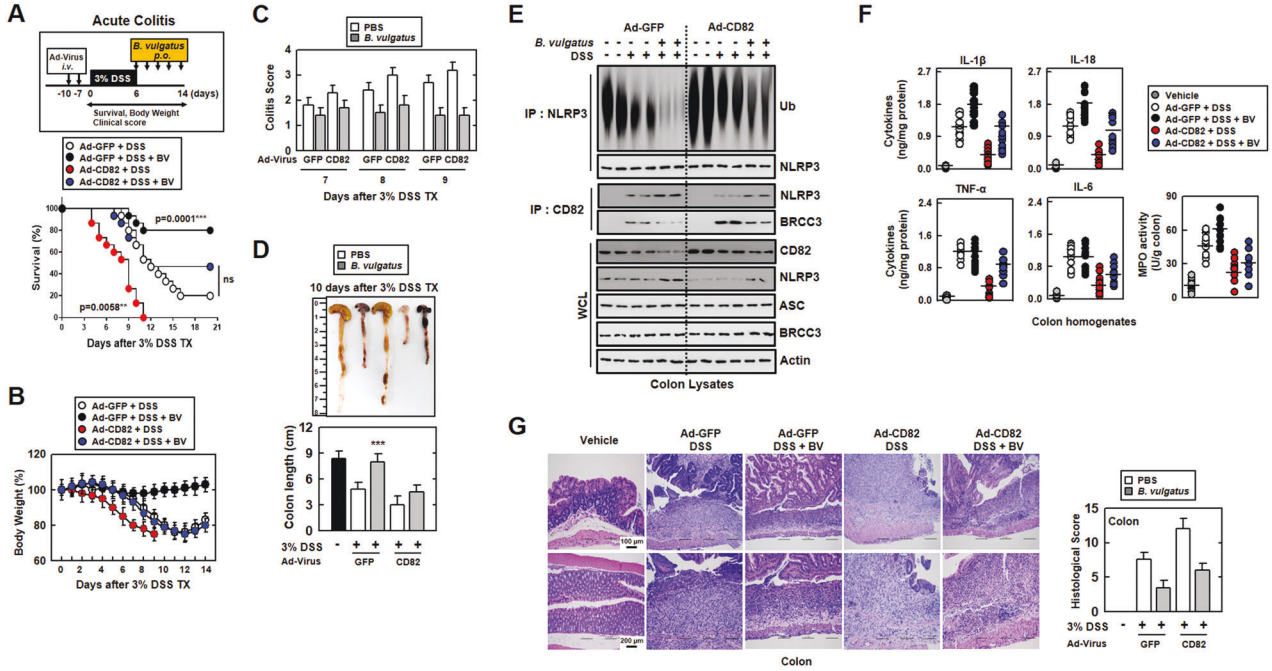

Fig. 8 ***B. vulgatus*** **exerts a therapeutic effect against acute DSS-induced colitis in mice A** Schematic showing the acute colitis model transduced with Ad-GFP or Ad-CD82 virus (1×10^9 cfu/kg) and treated with 3% DSS for 6 days and infected with *B. vulgatus* (2×10^7 cfu/kg) (upper). The survival of +mice was monitored for 21 days; mortality was measured for $n = 15$ mice per group (lower). Statistical differences compared with the Ad-GFP + DSS group are indicated (log-rank test). The data are representative of three independent experiments with similar results. **B** Weight loss ($n = 8$). **C** Colitis scores were obtained from clinical parameters (weight loss, stool consistency, and bleeding) ($n = 8$). **D** Image (upper) and length (lower) of the colon ($n = 8$). **E** Colon samples were used for IP with an αNLRP3 or αCD82 antibody, followed by IB with an αUb, αNLRP3 or αBRCC3 antibody. WCLs were used for IB with an αCD82, αNLRP3, αASC, αBRCC3 or αActin antibody. **F** The levels of cytokines and the MPO activity in colon homogenates ($n = 10$). **G** Representative imaging of H&E staining of the colon (left) ($n = 10$). Histopathology scores were obtained on the basis of H&E staining as described in the Methods (Materials and Methods). Statistical significance was determined by Student's *t*-test with Bonferroni adjustment (***$p < 0.001$) compared with Ad-GFP + DSS (**D**). **E** The data are representative of three independent experiments with similar results

NLRP3 expression was time increased with time in BMDMs. We also observed that CD82 interacted with NLRP3 and BRCC3 in *B. vulgatus*-infected BMDMs (Fig. 7B). Moreover, the secretion of IL-1β and IL-18 in the *B. vulgatus*-infected BMDMs increased in proportion to time (Fig. 7C). Additionally, investigations revealed that infecting *B. vulgatus* promoted the deubiquitination of NLRP3 in WT BMDMs but exerted no effect on NLRP3 deubiquitination in $CD82^{-/-}$ BMDMs (Fig. 7D). In CD82-overexpressing BMDMs, increasing CD82 led to decreased levels of NLRP3, IL-1β, and IL-18 in *B. vulgatus*-infected BMDMs (Fig. S6A). Therefore, to determine whether *B. vulgatus* specifically inhibited CD82 activity in macrophages, we infected BMDMs with *Lactobacillus reuteri* (*L. reuteri*). The amount of *L. reuteri* in the colon was increased in the DSS-treated mice but not in untreated $CD82^{-/-}$ mice, in contrast to the effects of *B. vulgatus*. Additionally, CD82 did not interact with NLRP3 or BRCC3 in *L. reuteri*-infected BMDMs (Fig. 7E). In addition, we infected LPS-primed BMDMs treated with ATP with *B. vulgatus*. In LPS-primed WT BMDMs treated with ATP, *B. vulgatus* infection in decreased the ubiquitination of NLRP3. However, in CD82-overexpressing BMDMs, although the ubiquitination of NLRP3 was enhanced by ATP treatment, cotreatment with ATP and *B. vulgatus* in LPS-primed BMDMs attenuated the ubiquitination of NLRP3. Correspondingly, although treatment of LPS-primed BMDMs with *B. vulgatus* inhibited CD82 expression and NLRP3 degradation (Fig. 7F), the levels of IL-1β and IL-18 were higher in *B. vulgatus*-ATP cotreated LPS-primed BMDMs (Fig. 7G). Subsequently, we examined whether *B. vulgatus* regulated CD82 by treating LPS-primed BMDMs with TAT-CD82 (aa 152–158). The results showed that although TAT-CD82 (aa 152–158) enhanced the ubiquitination of NLRP3, the addition of *B. vulgatus* diminished the ubiquitination of NLRP3 in the BMDMs. We also observed that the interaction between CD82 and BRCC3 was modulated by *B. vulgatus* treatment in TAT- or TAT-CD82 (aa 152–158)-treated BMDMs, and treatment with *B. vulgatus* increased IL-1β and IL-18 levels in the TAT-CD82 (aa 152–158)-treated BMDMs (Fig. S6B). Notably, the regulatory mechanism underlying changes in CD82 expression mediated by *B. vulgatus* directly affected CD82 DNA methylation. Bisulfite modification followed by methylation-specific PCR and pyrosequencing analysis allowed us to quantify CD82 methylation; macrophages treated with *B. vulgatus* exhibited markedly lower methylated CD82 levels and higher unmethylated CD82 levels between bp positions −127 and −286, and the effect was time dependent (Fig. S7A). *B. vulgatus* did not inhibit CD82 expression by promoting CD82 degradation (Fig. S7B). Furthermore, in *B. vulgatus*-treated macrophages, no change in NLRP3 or BRCC3 expression was found with or without MG-132 treatment (Fig. S8). Our studies suggest that *B. vulgatus* regulates only CD82 expression, and NLRP3 ubiquitination and degradation by BRCC3 were considered to be specifically dependent on NLRP3 inflammasome stimuli. These results demonstrated that *B. vulgatus* suppressed the expression of CD82 and increased the deubiquitination rate of NLRP3 by enhancing the activation of the NLRP3 inflammasome in macrophages.

B. vulgatus protects mice from DSS-induced colitis by mediating CD82-BRCC3-NLRP3 axis activation

We next investigated the protective role played by *B. vulgatus* in DSS-induced colitis in mice. First, we treated Ad-GFP or Ad-CD82 mice with 3% DSS for 6 days, and then we infected mice with *B. vulgatus*. In the WT mice, *B. vulgatus* infection significantly rescued the mice from DSS-induced colitis. Additionally, CD82-overexpressing mice were less susceptible to colitis after treatment with *B. vulgatus*

(Fig. 8A). Moreover, body weight loss was decreased in the *B. vulgatus*-treated WT and Ad-CD82 mice (Fig. 8B). We also observed that *B. vulgatus* treatment in DSS-treated mice alleviated the colitis score and increased the colon length (Fig. 8C, D). Hence, we evaluated the level of NLRP3 deubiquitination and the degree of binding between CD82 and NLRP3 or BRCC3 in the colon. In the Ad-GFP mouse colon, the ubiquitination of NLRP3 and expression of CD82 were decreased by an increase in NLRP3 level in the DSS- and *B. vulgatus*-treated groups. Similarly, although overexpressing CD82 increased the NLRP3 ubiquitination rate, infection with *B. vulgatus* reduced ubiquitinated NLRP3 through the blockade of the NLRP3-CD82 interaction (Fig. 8E). Additionally, the levels of cytokines were decreased in Ad-CD82 mice compared with control mice. However, supplemental *B. vulgatus* treatments increased the expression of cytokines in both DSS-treated Ad-GFP and Ad-CD82 mice, and an MPO activity analysis showed that *B. vulgatus* infection increased inflammation in mice (Fig. 8F). By H&E staining, we found that the histological score in the colon was decreased in *B. vulgatus*-treated mice with colitis (Fig. 8G). Furthermore, we validated the therapeutic value of *B. vulgatus* infection in a chronic colitis mouse model. The results showed that the increase in the survival time and sustained body weight of the mice depended on the number of *B. vulgatus* doses they received (Fig. S9). Altogether, these results demonstrated that *B. vulgatus* might regulate the pathogenesis of colitis by inhibiting the CD82-BRCC3-NLRP3 interaction.

DISCUSSION

In this research, we demonstrated the role of CD82 in the negative regulation of NLRP3 inflammasome activation mediated through its binding partners, including NLRP3 and BRCC3. Then, we assessed the contribution of CD82 to the pathogenesis of colitis. The major findings of this study are as follows: (1) CD82 specifically mediated the assembly of the NLRP3 inflammasome and the secretion of IL-1β and IL-18 in macrophages. (2) CD82 deficiency alleviated susceptibility to colitis by upregulating NLRP3-related inflammation in mice. (3) CD82 was directly associated with NLRP3 and BRCC3 in endosomal fractions of macrophages. (4) AA 152-158 in CD82 are essential for CD82 interaction with NLRP3 and BRCC3. (5) CD82 shows a higher affinity for BRCC3 than for NLRP3, and the interaction between CD82 and BRCC3 increased the degradation of NLRP3 by blocking BRCC3-dependent K63-specific deubiquitination of NLRP3. (6) *B. vulgatus* controlled CD82 expression by CD82 DNA hypomethylation and promoted the expression of IL-1β and IL-18 in BMDMs. (7) Administering *B. vulgatus* conferred protection against DSS-induced colitis onto mice by modulating the expression of CD82 and enhancing the inflammation induced by NLRP3. These observations collectively suggested that CD82 plays a crucial role in the regulation of the NLRP3 inflammasome and exerts a damaging effect on colitis. Moreover, this study established that the regulation of CD82 through gene silencing or treatment with *B. vulgatus* may be a potential therapeutic strategy against colitis because it favored the activation of the NLRP3 inflammasome in macrophages.

CD82 is a well-characterized tetraspanin located in the surface membrane and a fundamental regulator. As a tumor suppressor, it has been associated with various proteins, such as integrins, epidermal growth factor receptor (EGFR), EWI2/PGRL, KITENIN, and protein kinase C (PKC), in several cancers [36–40]. The most critical characteristic of CD82 in immune cells is its regulatory effect on leukocyte recruitment and migration in immune responses [41]. Recent studies have indicated that CD82 interacts with several integrins, including $\alpha_4\beta_1$, to promote adhesion to fibronectin, stability of $\alpha_4\beta_1$ at the cell surface, and assembly of $\alpha_4\beta_1$ clusters in a leukemic progenitor cell line [42, 43]. Similarly, we discovered that although full-length CD82 was directly related to NLRP3 and BRCC3 in macrophages, a region including amino acids 152–158 in the LEL domain of CD82 was identified as playing the essential role in the interaction of these proteins. CD82 LEL comprises six highly conserved cysteine residues that form disulfide bonds, making them important regions for the proper LEL structure. Many interactions with other proteins are mediated through to this region of CD82 [44–46]. Interestingly, the interaction between the LEL of CD82 and NLRP3 or BRCC3 in the cytosol and nuclear fraction was noted. Therefore, we speculated that CD82 was localized in the endosome membrane, endoplasmic reticulum, and phagosome, which might interact with cytosolic NLRP3 and BRCC3. However, how the LEL of CD82 is exposed to the cytosol to mediate the interaction with NLRP3 and BRCC3 remains to be clarified.

Inflammatory bowel disease (IBD), including Crohn's disease and UC, is caused by chronic and aggravated inflammation in the gastrointestinal tract, dysregulating the immune system. Aberrant innate immune responses in the colon are critical to elucidating the pathogenesis of IBD[47]. Studies have also reported that although the NLRP3 inflammasome is a crucial regulator of intestinal homeostasis, it can alleviate colitis by targeting the regulatory mechanism mediating NLRP3 inflammasome activation [48, 49]. Additionally, recent studies reported that the activation of the NLRP3 inflammasome confers protection against colitis, showing that IL-1β can increase the expression of IL-2, which prolongs the survival of T cells and reinforces the generation of antibodies by B cells [50, 51]. Furthermore, studies of a chemically induced colitis model reported that IL-1β protected mice from intestinal infection with *Citrobacter rodentium* and *Clostridium difficile* by preventing phagocytosis and eliminating bacteria in mononuclear phagocytes [29, 30]. A few other studies have also indicated that IL-18 confers protection against colitis and colitis-associated cancer [52–57]. Moreover, the activation of IFN-γ and downstream STAT-1 signaling, which depend on IL-18, was downregulated in NLRP3-deficient mice and inhibited the proliferation and repair of the injured epithelium in the intestinal tract [58]. In line with these findings, the present study revealed a protective role of CD82 deficiency in a colitis model during the activation of NLRP3. In addition, we observed that CD82 specifically conferred greater colitis sensitivity by interacting with BRCC3, regulating the degradation of NLRP3 via K63-specific deubiquitination. Alternatively, a number of studies have suggested that BRCC3 is a positive regulator of NLRP3 that promotes NLRP3 oligomerization via K63-specific deubiquitination at the LRR domain of NLRP3. Similarly, the present study showed that the N-terminus of BRCC3 interacts with CD82, and this interaction was shown to regulate the NLRP3 inflammasome with deleterious effects in DSS-induced colitis mice.

Subsequently, we investigated the colon microbiota of mice with colitis and observed that the proportion of *B. vulgatus* was significantly altered with specific changes in CD82 expression. Bacteroides is among of the most prevalent genera in the mammalian colon and is a potential probiotic candidate due to its role in regulating numerous disorders, such as obesity, diarrhea, viral encephalitis, and enteritis [58]. In previous studies, *B. vulgatus* has also been recognized as a representative species because of its favorable effects on human colon viability [59, 60]. Moreover, although one study indicated that *B. vulgatus* alleviated *Escherichia coli*-induced colitis or *Yersinia enterocolitica*-induced inflammation [61, 62], another study demonstrated that certain *B. vulgatus* species induced inflammation in transgenic rats with colitis [63]. A recent study showed that each *B. vulgatus* strain exerted a different effect [58]. In the present investigation, we specifically found that the proportion of *B. vulgatus* was increased in the colon microbiota of mice with DSS-induced colitis. Intriguingly, although increasing *B. vulgatus* levels mediated the level of CD82 and the interaction between CD82and BRCC3 by upregulating the NLRP3 inflammasome, the *L. reuteri* level, which has been shown to be increased in colitis, was found to be unrelated to CD82. These findings suggest that *B. vulgatus* can be used to develop a new therapeutic strategy by enhancing NLRP3 inflammasome activation and modulating the expression of CD82,

attenuating its interaction with BRCC3. Nevertheless, further studies on how *B. vulgatus* controls CD82 in colitis are necessary.

Collectively, our findings show that the regulation of CD82 exerts a protective effect against DSS-induced colitis in mice. Under inflammatory conditions,CD82 decreases the activation of the NLRP3 inflammasome by interacting with BRCC3 and blocking BRCC3-dependent K63-specific deubiquitination of NLRP3. Furthermore, we discovered that *B. vulgatus* was specifically related to the modulation of CD82 expression and its function. Moreover, the administration of *B. vulgatus* to mice increased survival and repaired colon viability in mice with colitis. Finally, this study demonstrated that the regulation of CD82 was vital in alleviating the pathology of colitis by enhancing NLRP3-related inflammation. Based on our findings, we propose that *B. vulgatus* is a potential therapeutic candidate that can regulate CD82 function to attenuate colitis.

MATERIALS AND METHODS

Mice and cell culture

$CD82^{-/-}$ and CD82-floxed mice were maintained on a C57BL/6 background as previously described [64]. LysMcre (B6.129P2-*Lyz2*$^{tm1(cre)Ifo}$/J, Strain # 004781) mice were obtained from the Jackson Laboratory. Wild-type C57BL/6 mice were purchased from Samtako Bio Korea (Gyeonggi-do, Korea). Primary bone marrow–derived macrophages (BMDMs) were isolated from $CD82^{+/+}$ and $CD82^{-/-}$ mice and cultured in DMEM for 3–5 days in the presence of M-CSF (R&D Systems, 416-ML), as described previously [65]. HEK293T cells (ATCC-11268; American Type Culture Collection) were cultured in DMEM (Gibco) containing 10% FBS (Gibco), sodium pyruvate, nonessential amino acids, penicillin G (100 IU/ml), and streptomycin (100 µg/ml). Human monocytic THP-1 cells (ATCC TIB-202) were grown in RPMI 1640/GlutaMAX supplemented with 10% FBS and treated with 20 nM PMA (Sigma–Aldrich) for 24 h to induce their differentiation into macrophage-like cells, and they were washed three times with PBS before use in experiments.

Reagents and antibodies

LPS (*Escherichia coli* O111:B4, tlrl-eblps), adenosine 5′-triphosphate (ATP, tlrl-atpl), nigericin, monosodium urate crystals (MSU, tlrl-msu), poly(dA:dT) (tlrl-patc) and flagellin (FLA-ST, tlrl-stfla) were purchased from Invivogen.

Antibodies specific for CD82 (TS82b) and BRCC3 (EPR4366) were purchased from Abcam. CD82 (C-16), actin (I-19), ASC (N-15-R), IL-18 (H-173-Y), caspase-1 p10 (M-20), lamin B1 (B-10), tubulin (5F131), Ub (P4D1), HA (12CA5), Flag (D-8), GST (B-14), Myc (9E10) and V5 (C-9) were purchased from Santa Cruz Biotechnology. Specific Abs against K63-poly-Ub (D7A11) and K48-poly-Ub (D9D5) were purchased from Cell Signaling Technology (Danvers, MA, USA). IL-1β (AF-401-NA) and NLRP3 (AG-20B-0014) were purchased from R&D Systems and Adipogen, respectively.

Plasmid construction

HA-tagged BRCC3, HA-tagged ubiquitin (Ub), K48-linkage-specific ubiquitin (K48-Ub), and K63-linkage-specific ubiquitin (K63-Ub) plasmids were purchased from Addgene. The plasmids encoding full-length CD82 or NLRP3 and mutant plasmids were previously described [64, 66]. Plasmids encoding different regions of BRCC3 (aa 1-316, 1-148, 149-228, 229-316) were generated by PCR amplification from full-length BRCC3 cDNA and subcloned into a pEBG derivative encoding an N-terminal GST epitope tag between BamHI and NotI sites. All constructs for transient transfection in mammalian cells were derived from a pEBG-GST mammalian fusion vector and a pEF-IRES-Puro expression vector. All constructs were sequenced using an ABI PRISM 377 automatic DNA sequencer to verify 100% correspondence with the original sequence.

Peptides

Tat-conjugated CD82 peptides were commercially synthesized and purified in acetate salt form to prevent abnormal responses in cells by Peptron (Korea). The amino acid sequences of the peptides in this study are described in Fig. 4. The endotoxin content, as measured by Limulus amebocyte lysate assay (BioWhittaker), was less than 3–5 pg/ml at the concentrations of the peptides used in the experiments.

GST pulldown, immunoblot, and immunoprecipitation analysis

THP-1 cells, 293 T cells, and BMDMs were treated as indicated and processed for analysis by GST pulldown, Western blotting and coimmunoprecipitation, as previously described [64–66]. For GST pulldown, 293 T cells were harvested and lysed in NP-40 buffer supplemented with a complete protease inhibitor cocktail (Roche, Basal, CH). After centrifugation, the supernatants were precleared with protein A/G beads at 4 °C for 2 h. Precleared lysates were mixed with a 50% slurry of glutathione-conjugated Sepharose beads (Amersham Biosciences, Amersham, UK), and for the binding reaction, this mixture was incubated for 4 h at 4 °C. Precipitates were washed extensively with lysis buffer. Proteins bound to glutathione beads were eluted with sodium dodecyl sulfate (SDS) loading buffer after boiling for 5 min. For immunoprecipitation, cells were harvested and then lysed in NP-40 buffer supplemented with a complete protease inhibitor cocktail (Roche, Basal, CH). After preclearing with protein A/G agarose beads for 1 h at 4 °C, whole-cell lysates were used for immunoprecipitation with the indicated antibodies. Generally, 1–4 µg of commercial antibody was added to 1 ml of cell lysate and incubated at 4 °C for 8 to 12 h. After the addition of protein A/G agarose beads and incubation for 6 h, the immunoprecipitates were extensively washed with lysis buffer and eluted with SDS loading buffer after boiling for 5 min. For immunoblotting (IB), polypeptides were resolved by SDS-polyacrylamide gel electrophoresis and transferred to a PVDF membrane (Bio–Rad, Hercules, CA, USA). Immunodetection was achieved with specific antibodies. Antibody binding was visualized by chemiluminescence (ECL; Millipore, Burlington, MA) and detected with a Vilber chemiluminescence analyzer (Fusion SL 3; Vilber Lourmat).

Enzyme-linked immunosorbent assay

Cell culture supernatants and mouse sera were analyzed for cytokine content using a BD OptEIA ELISA set (BD Pharmingen) for the detection of TNF-α, IL-6, IL-1β, and IL-18. All assays were performed as recommended by the manufacturer.

Interaction kinetic analyses of NLRP3 or BRCC3 with the CD82 binding partner

The interaction of CD82-NLRP3 or CD82-BRCC3 was monitored using a Fluoromax-4 spectrofluorometer (HORIBA Scientific) as previously described [67]. Briefly, NLRP3 or BRCC3 was labeled with BODIPY FL iodoacetamide (Thermo Fisher Scientific) according to the manufacturer's instructions. Labeled NLRP3 or BRCC3 was excited at 350 nm, and detection was performed through a cutoff filter at 512 nm. Fluorescently labeled NLRP3 or BRCC3 was titrated with unlabeled CD82 for a kinetic analysis. The excitation and emission wavelengths were 498 mm and 518 nm, respectively. The data obtained were fitted using the GraFit program. All fluorescence measurements were performed at 25 °C in 30 mM Tris, pH 7.4; 150 mM NaCl; and 1 mM dithiothreitol.

Injection of recombinant adenoviruses to express CD82 in mice

Recombinant adenoviruses (Ad-GFP and Ad-Rubicon) were injected intravenously via the tail vein at a dose of $\sim 5 \times 10^{12}$ pfu/mouse twice. Seven days post-transduction, the mice were challenged with 3% DSS (acute colitis). All animal-related procedures were reviewed and approved by the Institutional Animal Care and Use Committee of Hanyang University (protocol 2020-075).

Mouse model of colitis

DSS-induced acute or chronic colitis mouse models were prepared with 6-week-old C57BL/6 female mice (Samtako, Osan, Korea) as previously described [68]. To assess the induction of acute colitis, mice were given 3% (w/v) dextran sodium sulfate (molecular weight: 36,000–50,000 kDa, MP Biomedicals, Santa Ana, CA, USA) dissolved in drinking water with ad libitum access, as illustrated in Fig. 8A and 9. The DSS solutions were made freshly every 2 days. Control non-DSS-fed mice had access to sterile distilled water. The humane endpoint of the experiment was reached when the animals lost 20% of their body weight (compared to their original body weight), and then, the mice were euthanized. Body weight loss may not exceed 20% without an approved Exception request. All animal-related procedures were reviewed and approved by the

Institutional Animal Care and Use Committee of Hanyang University (protocol 2019–0081).

Clinical score and histology

For determining a clinical score of colitis, body weight, occult or gross blood lost per rectum, and stool consistency were measured every other day during colitis induction. The clinical score was assessed by two trained investigators blinded to the treatment groups [68]. For immunohistochemistry of tissue sections, mouse distal colon tissues were fixed in 10% formalin and embedded in paraffin. Paraffin sections (4 μm) were cut and stained with hematoxylin and eosin (H&E). For the histopathologic score, a board-certified pathologist (Dr. Min-Kyung Kim, Kim Min-Kyung Pathology Clinic, Seoul) independently scored each organ section without prior knowledge of the treatment groups, as previously described [68].

Preparation of bacterial strains

B. vulgatus (ATCC 8482) and *L. reuteri* (ATCC 23272) were obtained from the American Type Culture Collection (ATCC). The bacteria were cultured and prepared as single-cell suspensions as follows. Briefly, *B. vulgatus* was incubated at 37 °C with shaking in tryptic soy medium with 5% defibrinated sheep blood (ATCC Medium 260) under anaerobic conditions, and *L. reuteri* was incubated at 37 °C with shaking in lactobacilli MRS agar/broth (ATCC Medium 416) under aerobic conditions. All bacteria-related procedures were reviewed and approved by the Institutional Biosafety Committee of Hanyang University (HY-IBC-2021-01).

Miscellaneous procedures

Details of the protein ASC oligomerization assay, ASC pyroptosome purification, mass spectrometry, adenovirus construction and production, isolation of microbial DNA, 16 S rRNA gene-based amplicon sequencing, processing and analysis of sequencing data, methylation-specific polymerase chain reaction (MS-PCR), flow cytometry analysis of colon cells, and lentiviral shRNA production and transduction are provided in the Supporting Information.

Statistical analysis

All data were analyzed by Student's *t*-test with Bonferroni adjustment or ANOVA for multiple comparisons. The data are presented as the mean ± SD. Statistical analyses were performed using SPSS (Version 12.0) statistical software (SPSS, Chicago, IL, USA). Differences were considered significant when $p < 0.05$. For survival determinations, data were graphed and analyzed via the product limit method of Kaplan and Meier with the log-rank (Mantel-Cox) test performed using GraphPad Prism (version 5.0, La Jolla, CA, USA) for making comparisons.

DATA AVAILABILITY

This study includes no data deposited in external repositories.

REFERENCES

1. Gaugitsch HW, Hofer E, Huber NE, Schnabl E, Baumruker T. A new superfamily of lymphoid and melanoma cell proteins with extensive homology to Schistosoma mansoni antigen Sm23. Eur J Immunol. 1991;21:377–83.
2. Habibzadeh P, Honarvar B, Silawi M, Bahramjahan S, Kazemi A, Faghihi MA, et al. Association between rs2303861 polymorphism in CD82 gene and non-alcoholic fatty liver disease: a preliminary case-control study. Croat Med J. 2019;60:361–8.
3. Tam JM, Reedy JL, Lukason DP, Kuna SG, Acharya M, Khan NS, et al. Tetraspanin CD82 Organizes Dectin-1 into signaling domains to mediate cellular responses to Candida albicans. J Immunol. 2019;202:3256–66.
4. Wang G, Zhang L, Zhou Y, Sun Q, Xu H, Cai F, et al. KAI1/CD82 genetically engineered endothelial progenitor cells inhibit metastasis of human nasopharyngeal carcinoma in a mouse model. Med Sci Monit. 2018;24:3146–52.
5. Yan W, Huang J, Zhang Q, Zhang J. Role of metastasis suppressor KAI1/CD82 in different cancers. J Oncol. 2021;2021:9924473.
6. Khan NS, Lukason DP, Feliu M, Ward RA, Lord AK, Reedy JL, et al. CD82 controls CpG-dependent TLR9 signaling. Faseb J. 2019;33:12500–14.
7. Gil ML, Vita N, Lebel-Binay S, Miloux B, Chalon P, Kaghad M, et al. A member of the tetra spans transmembrane protein superfamily is recognized by a monoclonal antibody raised against an HLA class I-deficient, lymphokine-activated killer-susceptible, B lymphocyte line. Cloning preliminary Funct Stud, J Immunol. 1992;148:2826–33.
8. Fukudome K, Furuse M, Imai T, Nishimura M, Takagi S, Hinuma Y, et al. Identification of membrane antigen C33 recognized by monoclonal antibodies inhibitory to human T-cell leukemia virus type 1 (HTLV-1)-induced syncytium formation: altered glycosylation of C33 antigen in HTLV-1-positive T cells. J Virol. 1992;66:1394–401.
9. Nojima Y, Hirose T, Tachibana K, Tanaka T, Shi L, Doshen J, et al. The 4F9 antigen is a member of the tetra spans transmembrane protein family and functions as an accessory molecule in T cell activation and adhesion. Cell Immunol. 1993;152:249–60.
10. Artavanis-Tsakonas K, Kasperkovitz PV, Papa E, Cardenas ML, Khan NS, Van der Veen AG, et al. The tetraspanin CD82 is specifically recruited to fungal and bacterial phagosomes prior to acidification. Infect Immun. 2011;79:1098–106.
11. Vyas JM, Kim YM, Artavanis-Tsakonas K, Love JC, Van der Veen AG, Ploegh HL. Tubulation of class II MHC compartments is microtubule dependent and involves multiple endolysosomal membrane proteins in primary dendritic cells. J Immunol. 2007;178:7199–210.
12. Martinon F, Burns K, Tschopp J. The inflammasome: A molecular platform triggering activation of inflammatory caspases and processing of proIL-beta. Mol Cell. 2002;10:417–26.
13. Wang L, Manji GA, Grenier JM, Al-Garawi A, Merriam S, Lora JM, et al. PYPAF7, a novel PYRIN-containing Apaf1-like protein that regulates activation of NF-kappa B and caspase-1-dependent cytokine processing. J Biol Chem. 2002;277:29874–80.
14. Mangan MSJ, Olhava EJ, Roush WR, Seidel HM, Glick GD, Latz E. Targeting the NLRP3 inflammasome in inflammatory diseases. Nat Rev Drug Disco. 2018;17:688.
15. He Y, Hara H, Núñez G. Mechanism and regulation of NLRP3 inflammasome activation. Trends Biochem Sci. 2016;41:1012–21.
16. Huang Y, Xu W, Zhou R. NLRP3 inflammasome activation and cell death. Cell Mol Immunol. 2021;18:2114–27.
17. Bauernfeind FG, Horvath G, Stutz A, Alnemri ES, MacDonald K, Speert D, et al. Cutting edge: NF-kappaB activating pattern recognition and cytokine receptors license NLRP3 inflammasome activation by regulating NLRP3 expression. J Immunol. 2009;183:787–91.
18. Franchi L, Eigenbrod T, Núñez G. Cutting edge: TNF-alpha mediates sensitization to ATP and silica via the NLRP3 inflammasome in the absence of microbial stimulation. J Immunol. 2009;183:792–6.
19. Mariathasan S, Weiss DS, Newton K, McBride J, O'Rourke K, Roose-Girma M, et al. Cryopyrin activates the inflammasome in response to toxins and ATP. Nature. 2006;440:228–32.
20. Martinon F, Pétrilli V, Mayor A, Tardivel A, Tschopp J. Gout-associated uric acid crystals activate the NALP3 inflammasome. Nature. 2006;440:237–41.
21. Stutz A, Kolbe CC, Stahl R, Horvath GL, Franklin BS, van Ray O, et al. NLRP3 inflammasome assembly is regulated by phosphorylation of the pyrin domain. J Exp Med. 2017;214:1725–36.
22. Spalinger MR, Kasper S, Gottier C, Lang S, Atrott K, Vavricka SR, et al. NLRP3 tyrosine phosphorylation is controlled by protein tyrosine phosphatase PTPN22. J Clin Invest. 2016;126:1783–800.
23. Song N, Liu ZS, Xue W, Bai ZF, Wang QY, Dai J, et al. NLRP3 phosphorylation is an essential priming event for inflammasome activation. Mol Cell. 2017;68:185–197.
24. Py BF, Kim MS, Vakifahmetoglu-Norberg H, Yuan J. Deubiquitination of NLRP3 by BRCC3 critically regulates inflammasome activity. Mol Cell. 2013;49:331–8.
25. Zhou L, Liu T, Huang B, Luo M, Chen Z, Zhao Z, et al. Excessive deubiquitination of NLRP3-R779C variant contributes to very-early-onset inflammatory bowel disease development. J Allergy Clin Immunol. 2021;147:267–79.
26. Segata N, Izard J, Waldron L, Gevers D, Miropolsky L, Garrett WS, et al. Metagenomic biomarker discovery and explanation. Genome Biol. 2011;12:R60.
27. Ordás I, Eckmann L, Talamini M, Baumgart DC, Sandborn WJ. Ulcerative colitis. Lancet. 2012;380:1606–19.
28. Yao X, Zhang C, Xing Y, Xue G, Zhang Q, Pan F, et al. Remodelling of the gut microbiota by hyperactive NLRP3 induces regulatory T cells to maintain homeostasis. Nat Commun. 2017;8:1896.
29. Hasegawa M, Kamada N, Jiao Y, Liu MZ, Núñez G, Inohara N. Protective role of commensals against Clostridium difficile infection via an IL-1β-mediated positive-feedback loop. J Immunol. 2012;189:3085–91.
30. Alipour M, Lou Y, Zimmerman D, Bording-Jorgensen MW, Sergi C, Liu JJ, et al. A balanced IL-1β activity is required for host response to Citrobacter rodentium infection. PLoS One. 2013;8:e80656.
31. Shao G, Lilli DR, Patterson-Fortin J, Coleman KA, Morrissey DE, Greenberg RA. The Rap80-BRCC36 de-ubiquitinating enzyme complex antagonizes RNF8-Ubc13-dependent ubiquitination events at DNA double strand breaks. Proc Natl Acad Sci USA. 2009;106:3166–71.
32. Shao G, Patterson-Fortin J, Messick TE, Feng D, Shanbhag N, Wang Y, et al. MERIT40 controls BRCA1-Rap80 complex integrity and recruitment to DNA double-strand breaks. Genes Dev. 2009;23:740–54.

33. Sobhian B, Shao G, Lilli DR, Culhane AC, Moreau LA, Xia B, et al. RAP80 targets BRCA1 to specific ubiquitin structures at DNA damage sites. Science. 2007;316:1198–202.
34. Ling J, Su J, Ma Z, Ruan C. The WXXW motif in the TSR1 of ADAMTS13 is important for its secretion and proteolytic activity. Thromb Res. 2013;131:529–34.
35. Hamilton PT, Jansen MS, Ganesan S, Benson RE, Hyde-Deruyscher R, Beyer WF, et al. Improved bone morphogenetic protein-2 retention in an injectable collagen matrix using bifunctional peptides. PLoS One. 2013;8:e70715.
36. Odintsova E, Sugiura T, Berditchevski F. Attenuation of EGF receptor signaling by a metastasis suppressor, the tetraspanin CD82/KAI-1. Curr Biol. 2000;10:1009–12.
37. Zhang XA, Bontrager AL, Hemler ME. Transmembrane-4 superfamily proteins associate with activated protein kinase C (PKC) and link PKC to specific beta(1) integrins. J Biol Chem. 2001;276:25005–13.
38. Lee JH, Park SR, Chay KO, Seo YW, Kook H, Ahn KY, et al. interacting tetraspanin (KITENIN), a member of the tetraspanin family, interacts with KAI1, a tumor metastasis suppressor, and enhances metastasis of cancer. Cancer Res. 2004;64:4235–43.
39. Zhang XA, He B, Zhou B, Liu L. Requirement of the p130CAS-Crk coupling for metastasis suppressor KAI1/CD82-mediated inhibition of cell migration. J Biol Chem. 2003;278:27319–28.
40. Zhang XA, Lane WS, Charrin S, Rubinstein E, Liu L. EWI2/PGRL associates with the metastasis suppressor KAI1/CD82 and inhibits the migration of prostate cancer cells. Cancer Res. 2003;63:2665–74.
41. Yeung L, Hickey MJ, Wright MD. The many and varied roles of tetraspanins in immune cell recruitment and migration. Front Immunol. 2018;9:1644.
42. Mannion BA, Berditchevski F, Kraeft SK, Chen LB, Hemler ME. Transmembrane-4 superfamily proteins CD81 (TAPA-1), CD82, CD63, and CD53 specifically associated with integrin alpha 4 beta 1 (CD49d/CD29). J Immunol. 1996;157:2039–47.
43. Miranti CK. Controlling cell surface dynamics and signaling: How CD82/KAI1 suppresses metastasis. Cell Signal. 2009;21:196–211.
44. Hemler ME. Specific tetraspanin functions. J Cell Biol. 2001;155:1103–7.
45. Stipp CS, Kolesnikova TV, Hemler ME. Functional domains in tetraspanin proteins. Trends Biochem Sci. 2003;28:106–12.
46. Liu WM, Zhang XA. KAI1/CD82, a tumor metastasis suppressor. Cancer Lett. 2006;240:183–94.
47. Zhen Y, Zhang H. NLRP3 inflammasome and inflammatory bowel disease. Front Immunol. 2019;10:276.
48. Guarda G, So A. Regulation of inflammasome activity. Immunology. 2010;130:329–36.
49. Zhu S, Ding S, Wang P, Wei Z, Pan W, Palm NW, et al. Nlrp9b inflammasome restricts rotavirus infection in intestinal epithelial cells. Nature. 2017;546:667–70.
50. Sahoo M, Ceballos-Olvera I, del Barrio L, Re F. Role of the inflammasome, IL-1β, and IL-18 in bacterial infections. ScientificWorldJournal. 2011;11:2037–50.
51. Mahida YR, Wu K, Jewell DP. Enhanced production of interleukin 1-beta by mononuclear cells isolated from mucosa with active ulcerative colitis of Crohn's disease. Gut. 1989;30:835–8.
52. Oficjalska K, Raverdeau M, Aviello G, Wade SC, Hickey A, Sheehan KM, et al. Protective role for caspase-11 during acute experimental murine colitis. J Immunol. 2015;194:1252–60.
53. Allen IC, TeKippe EM, Woodford RM, Uronis JM, Holl EK, Rogers AB, et al. The NLRP3 inflammasome functions as a negative regulator of tumorigenesis during colitis-associated cancer. J Exp Med. 2010;207:1045–56.
54. Engler DB, Leonardi I, Hartung ML, Kyburz A, Spath S, Becher B, et al. Helicobacter pylori-specific protection against inflammatory bowel disease requires the NLRP3 inflammasome and IL-18. Inflamm Bowel Dis. 2015;21:854–61.
55. Ratsimandresey RA, Indramohan M, Dorfleutner A, Stehlik C. The AIM2 inflammasome is a central regulator of intestinal homeostasis through the IL-18/IL-22/STAT3 pathway. Cell Mol Immunol. 2017;14:127–42.
56. Seregin SS, Golovchenko N, Schaf B, Chen J, Eaton KA, Chen GY. NLRP6 function in inflammatory monocytes reduces susceptibility to chemically induced intestinal injury. Mucosal Immunol. 2017;10:434–45.
57. Itani S, Watanabe T, Nadatani Y, Sugimura N, Shimada S, Takeda S, et al. NLRP3 inflammasome has a protective effect against oxazolone-induced colitis: a possible role in ulcerative colitis. Sci Rep. 2016;6:39075.
58. Zaki MH, Boyd KL, Vogel P, Kastan MB, Lamkanfi M, Kanneganti TD. The NLRP3 inflammasome protects against loss of epithelial integrity and mortality during experimental colitis. Immunity. 2010;32:379–91.
59. Qin J, Li R, Raes J, Arumugam M, Burgdorf KS, Manichanh C, et al. A human gut microbial gene catalogue established by metagenomic sequencing. Nature. 2010;464:59–65.
60. Tap J, Mondot S, Levenez F, Pelletier E, Caron C, Furet JP, et al. Towards the human intestinal microbiota phylogenetic core. Environ Microbiol. 2009;11:2574–84.
61. Waidmann M, Bechtold O, Frick JS, Lehr HA, Schubert S, Dobrindt U, Loeffler J, et al. Bacteroides vulgatus protects against Escherichia coli-induced colitis in gnotobiotic interleukin-2-deficient mice. Gastroenterology. 2003;125:162–77.
62. Frick JS, Fink K, Kahl F, Niemiec MJ, Quitadamo M, Schenk K, et al. Identification of commensal bacterial strains that modulate Yersinia enterocolitica and dextran sodium sulfate-induced inflammatory responses: Implications for the development of probiotics. Infect Immun. 2007;75:3490–7.
63. Rath HC, Wilson KH, Sartor RB. Differential induction of colitis and gastritis in HLA-B27 transgenic rats selectively colonized with Bacteroides vulgatus or Escherichia coli. Infect Immun. 1999;67:2969–74.
64. Koh HJ, Kim YR, Kim JS, Yun JS, Kim S, Kim SY, et al. CD82 hypomethylation is essential for tuberculosis pathogenesis via regulation of RUNX1-Rab5/22. Exp Mol Med. 2018;50:1–15.
65. Kim SY, Kim D, Kim S, Lee D, Mun SJ, Cho E, et al. Mycobacterium tuberculosis Rv2626c-derived peptide as a therapeutic agent for sepsis. EMBO Mol Med. 2020;12:e12497.
66. Kim JS, Mun SJ, Cho E, Kim D, Son W, Jeon HI, et al. Toxoplasma gondii GRA9 regulates the activation of NLRP3 inflammasome to exert anti-septic effects in mice. Int J Mol Sci. 2020;21:8437.
67. Guo Z, Ahmadian MR, Goody RS. Guanine nucleotide exchange factors operate by a simple allosteric competitive mechanism. Biochemistry. 2005;44:15423–9.
68. Kim JS, Kim YR, Jang S, Wang SG, Cho E, Mun SJ, et al. Mito-TIPTP increases mitochondrial function by repressing the Rubicon-p22phox interaction in colitis-induced mice. Antioxidants (Basel). 2021;10:1954.

ACKNOWLEDGEMENTS

This work was supported by the NRF grant funded by the Korean government (MSIP) (2021R1A4A5032463) and the research fund of Hanyang University (HY-2021). We thank all members of the Infection Biology Laboratory for critical reading and discussion of the manuscript.

AUTHOR CONTRIBUTIONS

JSK, HKK, SJ, EC, and SJM performed molecular and animal experiments and analyzed the data. JL and SY analyzed the pyrosequencing data. CSY designed and conceptualized the research, supervised the experimental work, analyzed the data, and wrote the manuscript.

COMPETING INTERESTS

The authors declare no competing interests.

ADDITIONAL INFORMATION

Supplementary information The online version contains supplementary material available at https://doi.org/10.1038/s41423-022-00971-1.

Correspondence and requests for materials should be addressed to Chul-Su Yang.